SIMULATION OF RADIOWAVE PROPAGATION USING PROPAGATION MODELS

Yelena Chaiko
Transport Communications and Information Systems professor group
Riga Technical University Institute of Railway Transport
Indrika, LV-1004, Riga, Latvia
E-mail: krivcha@inbox.lv

KEYWORDS
Model, propagation channel, radio communication system, pathloss, base station, simulation.

ABSTRACT

In this article we review the fundamental issues involving the simulation of the radio channel and discuss some of the more challenging simulation topics that are pertinent to the radio channel.

Radio and propagation channels

The propagation channel, together with the transmit and receive antennas, constitute the *radio channel*. Figure 1 depicts the propagation and radio channel's place in a radio communication system.

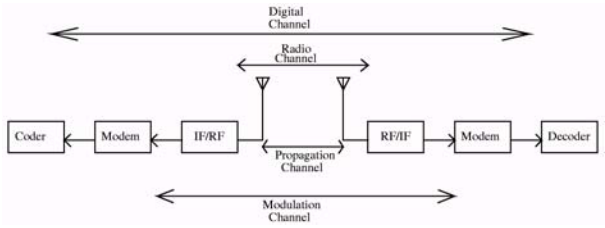

Figures 1: Various channels in a communications system.

The net effect of reflection, diffraction and scattering on the transmitted signal is attenuation, delay and phase change. Formally, this can be seen by starting from examination of the familiar wave equation

$$\frac{\partial^2\phi}{\partial x^2}+\frac{\partial^2\phi}{\partial y^2}+\frac{\partial^2\phi}{\partial z^2}=\frac{1}{c^2}\frac{\partial^2\phi}{\partial t^2} \qquad (1)$$

which describes the propagation of waves. The wave equation has the well-known plane-wave solution which in one dimension (corresponding to horizontal propagation of vertically polarized field) is given by:

$$\varphi(\mathrm{x},\mathrm{t})=S(x,t)e^{j\omega_c(t-x/c)} \qquad (2)$$

where *s(x,t)* is the information bearing (or complex envelope) of the wave propagating in the *x* direction and ω_c the carrier frequency in radian/sec. Letting the delay $\tau = x/c$ and making the spatial dependency *x* implicit we have

$$\varphi(\mathrm{t},\tau)=\left[S(t-\tau)e^{-j\omega_c\tau}\right]e^{j\omega_c t} \qquad (3)$$

In a multipath environment, *r(t),* the complex low-pass representation of the received signal is the contribution of many rays:

$$r(t)=\sum_n \alpha_n(t)S(t-\tau_n(t))e^{-j\omega_c\tau_n(t)} \qquad (4)$$

where $\alpha_n(t)$ denotes the time varying complex amplitude of the nth ray. Note that in addition to the time varying amplitudes $\alpha_n(t)$, the delay of each path is also a function of time. Equivalently, the RF equivalent counterparts of r(t) and s(t) denoted by S(t) and R(t) are

$$S(t)=\mathrm{Re}\left\{S(t)e^{j\omega_c t}\right\}$$

$$R(t)=\Re\left\{\sum_n \alpha_n(t)S(t-\tau_n(t))e^{j\omega_c(t-\tau_n(t))}\right\} \qquad (5)$$

Signal impairments

Communication quality between a base station and mobile or portable transceiver depends, among other factors, on the type and degree of impairments the signal undergoes in the radio channel. These impairments are now reasonably well understood and hence need to be included as essential parts of a realistic radio channel model. Some of the more important impairments are:

1. Pathloss
The transmitted signal suffers a loss proportional to $1/R^n$ where *R* is the distance between transmit and receive antennas and *n* is a positive number typically between 2 and 6. For free space transmission, $n = 2$ and the free space pathloss is given (in dB) by

$$L_{FS} = +20\log_{10}f_c+20\log_{10}R+32.4 \qquad (6)$$

Proceedings 19th European Conference on Modelling and Simulation
Yuri Merkuryev, Richard Zobel, Eugène Kerckhoffs © ECMS, 2005
ISBN 1-84233-112-4 (Set) / ISBN 1-84233-113-2 (CD)

where R is distance between transmit and receive antennas (in km) and fc is the carrier frequency in MHz. Although free-space assumption is quite optimistic, it provides a useful figure of reference for pathloss.

There are a number of more useful pathloss models for the propagation channel that are based on either theory, extensive measurements, or both. One such model is the analytical "flat earth" two-ray model that assumes a direct and a reflected ray coming from the ground as illustrated in Figure 2. This model takes into account the antenna heights, polarization of waves and the complex reflection coefficient of the earth surface.

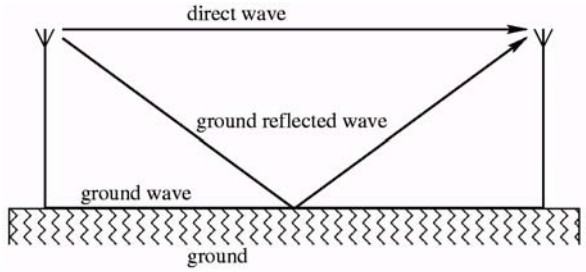

Figures 2: The two ray, flat earth model.

In this model, there are two regions with different slopes separated by a breakpoint, beyond which the pathloss follows a $1/R^4$ law or 6 dB per octave. In the first region, however, the received signal oscillates due to destructive and constructive addition of the two rays. This phenomena can be described by the Fresnel zone clearance, where the breakpoint can be viewed as the distance for which the ground just begins to obstruct the first Fresnel zone. Figure 3 depicts the pathloss based on the flat-earth model as the mobile drives away from the base station with a constant velocity. The x-axis can be viewed as distance between MS and BTS.

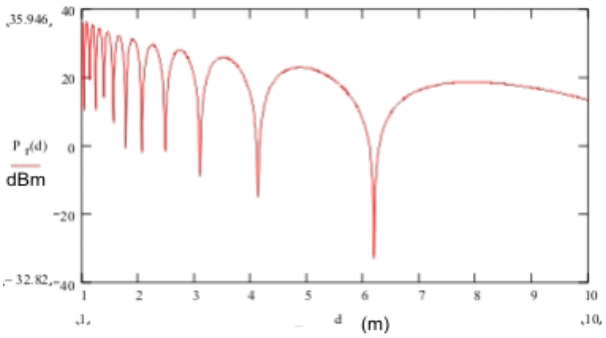

Figures 3: Losses of capacity of a signal in a point of reception P (d) (dBm) as function from distance d (m).

A measurement-based model for pathloss in the mobile environment has been developed by Hata [1]. This model was developed from extensive data gathered by Okumura [2]. Hata's model predicts pathloss in urban, suburban and rural areas and have antenna heights and frequency as parameters. Figure 4 shows the comparison of Hata's pathloss models for different environments as a function of distance (or time).

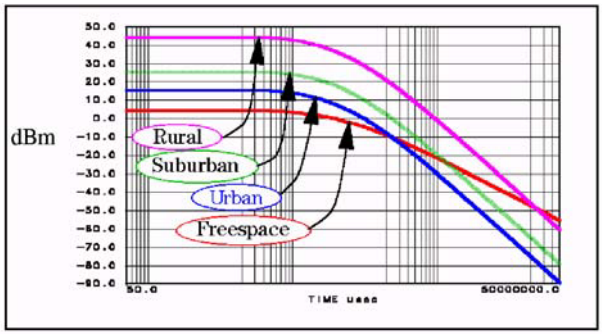

Figures 4: Comparison of Hata's pathloss models for different environments.

Simulation of radio channel

Today, simulation is increasingly replacing extensive and costly field measurements. The use of productivity tools, such as OmniSys, has merits over hardware channel simulators particularly during the design stages because it allows the user to study the radio channel interaction with RF/IF front end and modems without need for a costly and difficult hardware interface.

There are numerous models of propagation medium based on analytical and empirical studies. In general, these models can be classified as deterministic and statistical. Deterministic models are useful for predicting the signal strength at different locations and in presence of obstacles. These techniques have also the added advantage of being able to incorporate the effect of antenna radiation patterns as well as polarization of the fields. Deterministic approaches like Geometric Theory of Diffraction (GTD) , Uniform Theory of Diffraction (UTD) or Ray Tracing, are computationally intensive and require physical environment data. In spite of promising results, particularly for indoor environments, none of the deterministic modeling approaches have gained the flexibility or computational speed to be incorporated into an overall simulation of the digital channel. In addition, both GTD and UTD have serious limitations for predicting signal level in outdoor macrocell environments.

Statistical models treat the physical attributes of the medium as processes with certain distributions generally derived from measurements, deduction or both. Consequently, statistical models do not provide the user with accurate quantitative measure of the signal. Rather, they provide qualitative description of signals such as fluctuations, fade margins and the rate and duration of signal impairments. These models are ideal when a system perspective is sought. Common examples would be the performance evaluation of a given equalizer under frequency selective fading conditions or that of an AGC or power control loop as the signal degrades due to a flat fade or interference.

Propagation models

The (low-pass) impulse response of the propagation channel h(τ,t), characterized by several discrete paths, each having a specific delay and attenuation, can be deduced from equation (4) as

$$h(\tau,t)=\sum_n \alpha_n(t)e^{j\theta_n(t)}\delta(\tau-\tau_n(t)) \qquad (6)$$

If h(τ,t) is modeled as a zero mean Gaussian process, the envelope |h(τ,t)| at any time is Rayleigh-distributed. The transform of h(τ,t) with respect to time, gives the spectrum of time variation *S*(τ, v), generally referred to as delay-Doppler-spread function [1].
It has been shown [5] that for the case of two vertically polarized transmit and receive antennas and horizontal propagation of plane waves, *S*(τ, v) for a fixed delay (Doppler spectrum) is given by

$$S(\nu)=\frac{1}{2\pi\nu_m\sqrt{1-\left(\frac{\nu}{\nu_m}\right)^2}} \qquad \nu\le|\nu_m| \qquad (7)$$

where $\nu_m=\frac{V}{c}f_c$ is the maximum Doppler shift due to vehicle speed V. When a direct path exists such that the total multipath contribution is equal to that of the direct path the spectrum is Rician and is given by

$$S(\nu)=\frac{k_1}{2\pi\nu_m\sqrt{1-\left(\frac{\nu}{\nu_m}\right)^2}}+k_2\delta(\nu-k_3\nu_m) \qquad \nu\le|\nu_m| \qquad (8)$$

with k_1, k_2, k_3 constants related to proportion of direct and scattered signal and the direct wave angle of arrival.

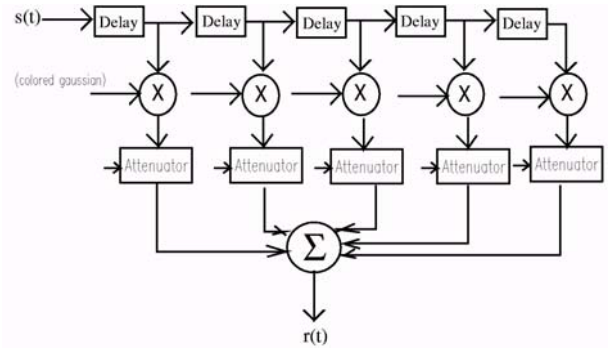

Figures 5: Tapped delay line channel model with frequency selective and flat fading.

A multipath fading model can therefore be constructed using a tapped-delay line filter. The typical tapped-delay line filter model for simulation is represented in Figure 5. To generate a Rayleigh fading profile for each path, independent added white Gaussian noise (AWGN) sources, in cascade with a filter representing the effects of Doppler spread can be used.

Cellular layout

Cellular layout typically involves the frequency reuse factor which is inversely proportional to K (number of cells per cluster). Figure 6a depicts the cellular layout with K=7 for a TDMA system. The shaded cells use the same frequency plan. The co-channel interference (CCI) is the most serious problem in this scheme while adjacent-channel interference is usually not a problem. D and R decide the interference levels where R is the radius of a cell and D the distance from center of a cell to its adjacent cell with the same frequency plan, as shown in the figure. D and R and number of cells in a cluster are related by D/R=$\sqrt{3}$K.

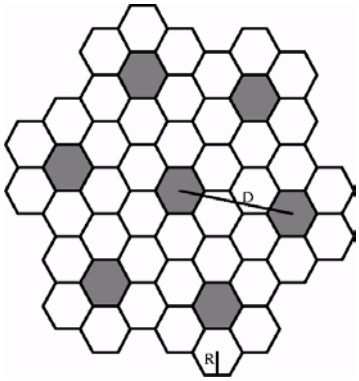

Figures 6a: Cellular layout for frequency reuse.

In spread spectrum systems (such as IS-95 CDMA) there is no frequency reuse and all cells use the same frequency band. This is possible because of the processing gain (21 dB) obtained by the use of quasi-orthogonal codes. In CDMA, mobiles are power controlled to equal power at cell site.

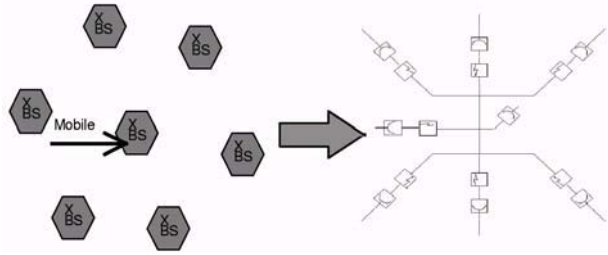

Figures 6b: Co-channel interference setup with equivalent schematic in OmniSys software.

In TDMA cellular applications, the designer should also make sure that the power level at the cell boundaries is weak enough not to spill over into the adjacent cells. By placing a home base station at the center and the interfering stations on the perimeter of a circle of radius D, one can simulate the received signal plus co-channel

interference at the mobile antenna coming from its own and interfering base stations or what is known as forward CCI. Figure 6b depicts this cell arrangements and its schematic representation. Forward CCI becomes significant when the path between the mobile and its own base is obstructed such that the desired signal is very weak. This scenario occurs particularly around the boundaries of cells. Figure 6c shows the received signal power for three different values of R as the mobile moves from the left edge of the cell with a velocity of 100 km/hr towards the right. These simulation results show that the interference level grows near the cell edges and beyond the cell boundaries. The simulation also shows that the interference level changes with the cell radius.

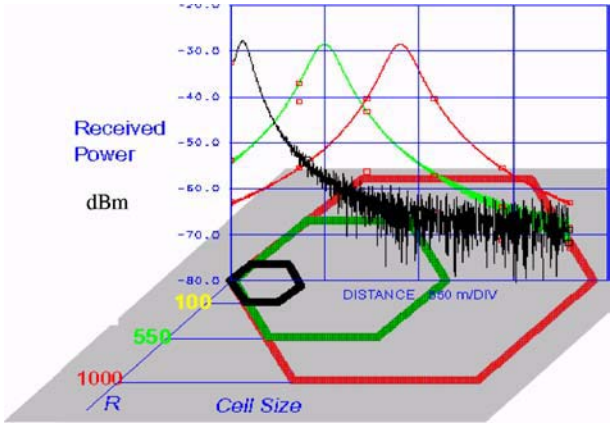

Figures 6c: Received signal power for three different values of D.

The change in signal to interference ratio (C/I) as a function of time as a mobile travels is a parameter of interest. Figure 7a depicts the setup, where a mobile is traveling from a home cell towards a co-channel cell in an urban environment. The C/I ratio is shown in Figure 7b as a function of time for various values of R. As shown, the C/I ratio is about 50 dB near the home base station and drops drastically as mobile moves toward the interfering base station.

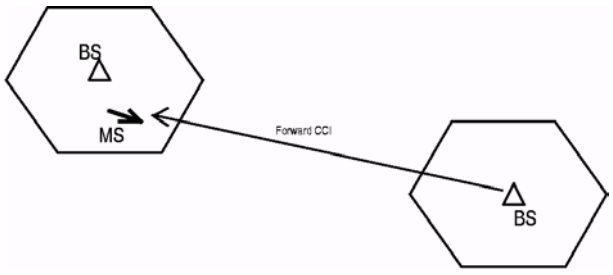

Figures 7a: A mobile traveling from a home cell towards a co-channel cell in an urban environment.

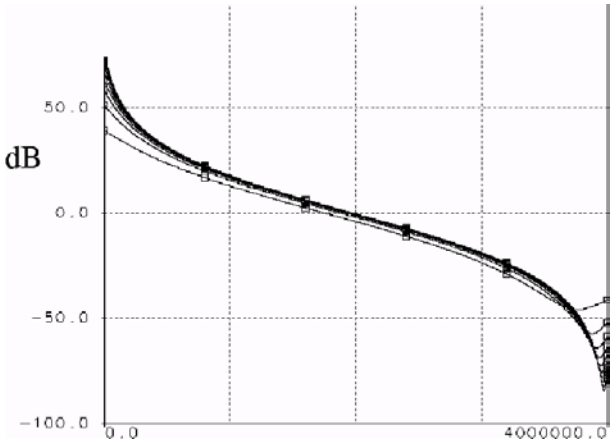

Figures 7b: C/I ratio as a function of time or distance.

Diversity and Combining

Antenna diversity is one of the methods for mitigating the fading signals. Space diversity relies on the fact that spatial fades occur about half a wavelength apart. Diversity reception relies on receiving a signal by combining two or more signals having very little correlation. The antennas are placed far enough such that the fade experienced by one antenna is not experienced by the other. Equivalently, since the rate, location and depth of fades is a function of carrier frequency, the transmission of two or more frequencies spaced far enough apart so that they are resolvable beyond duration of a fade constitutes frequency diversity.

There are basically two types of diversity reception, namely pre-detection and post-detection combining. Pre-detection combining is done via co-phasing of the randomly faded received signals or by picking the strongest signal among branches. Figure 8a depicts a reverse link design for reducing the fade margin by using a switched combining scheme. The mobile transmitter consists of a data source, GMSK modulator and the mobile antenna transmitting into the GSM propagation channel. The base station antenna system includes three omnidirectional antennas with a three-branch selection-combining scheme that includes two switches. The switch design is not described here, however it suffices to say that its function is to pick the signal with the stronger signal.

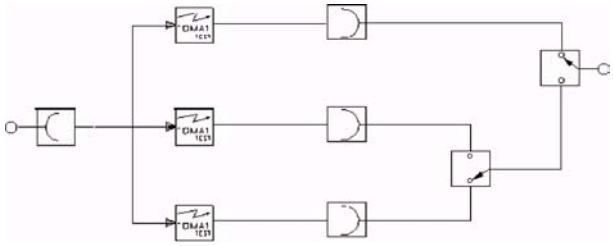

Figures 8a: Switched combining scheme for reducing the fade margin.

The upper trace in Figure 8b depicts the output of two antennas as well as the switch output. The lower trace shows the switching action for selecting either antenna. The output of the switch follows the stronger signal and hence avoids the deep fades of a single antenna. Figure 8c compares the cumulative probability density function (CDF) of one, two and three branch combining schemes, and Figure 8d depicts the average power from the two and three branch combiners, which shows a gain of up to three dB.

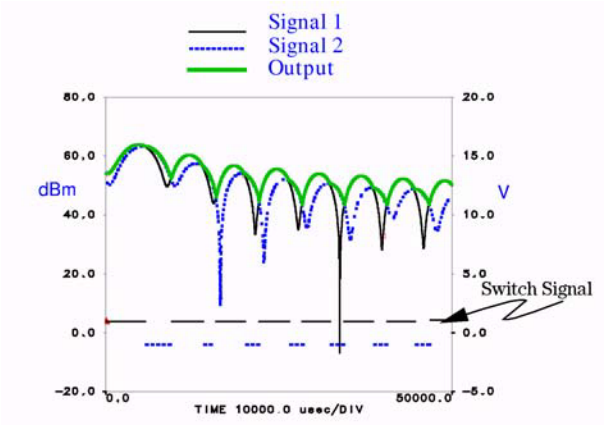

Figures 8b: Envelope of the switch input and output signals.

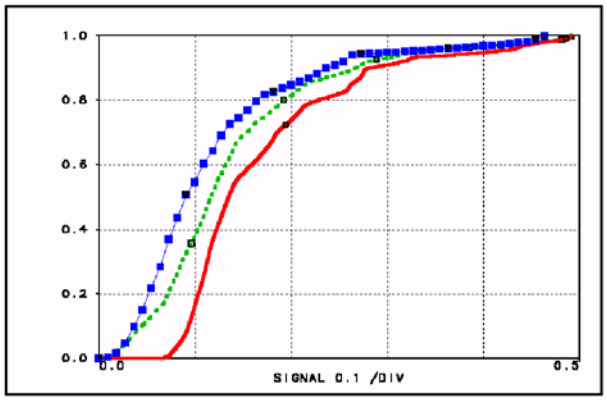

Figures 8c: Cumulative probability density function.

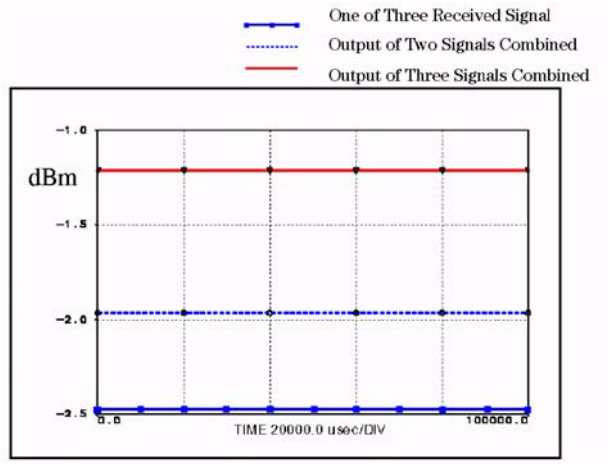

Figures 8d: Average power.

BER Simulations

BER simulation for AWGN channels are well studied and documented while less effort has been spent on the study of BER for fading channels. Such simulations enable the wireless designer to test the performance of various modulation schemes under harsh fading conditions. In the following examples we use a number of BER simulation focusing on P i/4 DQPSK and GMSK modulation schemes used in IS-54 and GSM systems for various fading conditions.

Figure 9a depicts the design setup for simulating an interference-limited channel with Pi/4 DQPSK modem. The interference limited assumption allows us to ignore AWGN and thereby concentrate on modeling the multipath fading in the presence of CCI. The simulation blocks include two identical but uncorrelated paths: one for the signal and the other for the interference. The signal and interference paths include a binary pseudo-random source, a Pi/4 DQPSK modulator, a mobile antenna moving with a fixed velocity as a parameter, an IS-54 (TDMA) propagation channel model with flat and two-ray frequency-selective options, base station antenna, and a coherent Pi/4 DQPSK demodulator including a carrier recovery. Note that two receive antennas are used for simulation to gauge the signal and interference separately, while in reality one antenna is used.

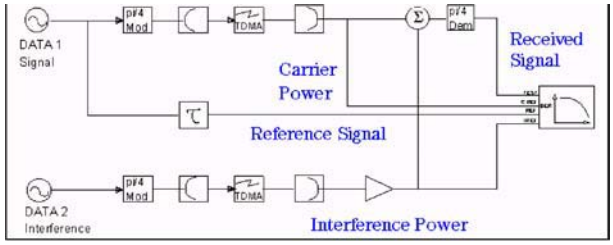

Figures 9a: An OmniSys simulation of an IS-54 system including fading radio channel with CCI.

The inputs to the modulator are the I and Q data streams in nonreturn to zero (NRZ) format. The NRZ data

symbols are differentially encoded for the Pi/4 DQPSK format, filtered with raised cosine filters, and then modulated to the carrier frequency with a QAM modulator.

The IS-54-based two-ray propagation channel impulse response is a special case of equation (7) described by

$$h(t,\tau)=\alpha_1(t)e^{j\theta_1}\delta(\tau-\tau_1)+\alpha_2(t)e^{j\theta_2}\delta(\tau-\tau_2) \quad (9)$$

Note that this model in general can be a flat fade (α_2 =0) or frequency selective depending on the way amplitudes and delays are specified. We use this model to simulate the BER for both flat and frequency selective fading conditions. The coherent Pi/4 DQPSK demodulator uses a carrier recovery scheme to recover a reference carrier signal. The modulated signal and the reference carrier are fed into a QPSK demodulation scheme that recovers I and Q components of the signal, pass it through a square root raised cosine filter and finally a differential decoder to produce the binary data signals.

A BER measurement compares the transmitted bit stream with the received signal after it is demodulated. First simulation uses a data stream (48.6 Kbits/s) over a flat fading channel. The output of this channel is added to that of the interfering signal, which is a different pseudo-random stream modulated and transmitted over a statistically independent channel. The same data rate is used for the interfering signal but the interference power is changed, resulting in different values of C/I. Figure 9b depicts the BER performance at four different mobile velocities (5, 30, 70 and 100 km/hr) corresponding to Doppler frequencies of 4.58, 27.52, 64.21, and 91.73 Hz at 990 MHz. The BER simulation was performed with a time step of a tenth of a bit or roughly 2 microseconds and a total of 20,000 bits were processed in the simulation.

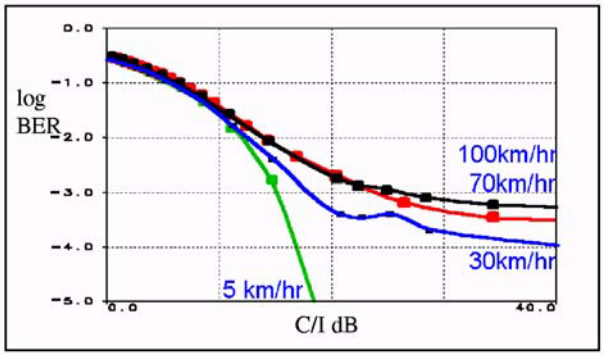

Figures 9b: OmniSys simulation of BER vs. C/I in NADC (IS-54) flat fading channel for different mobile speeds.

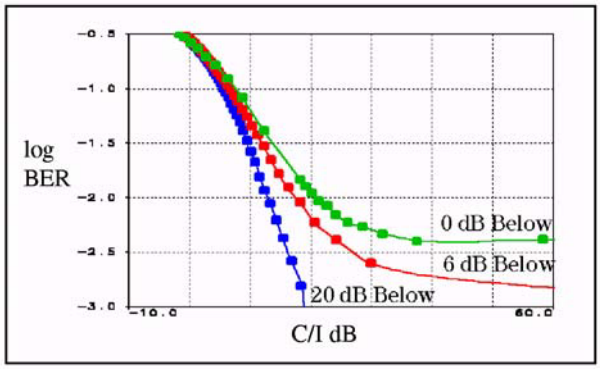

Figures 9c: OmniSys simulation of BER vs. C/I for different ratios of 1st over 2nd ray powers.

By fixing the mobile speed to 30 km/hr and using two-ray frequency-selective fading, the effect of power level in the second path can be simulated. The delay of the second path is set to a tenth of bit time. Figure 9c shows the BER simulation for various power levels of the second path with respect to the first. Figure 9d depicts BER as a function of C/I for various values of second path delay. Here, the power level on the second path is kept at 9 dB below the first, while the mobile travels at a very low speed (1 km/hr). Note that % delay refers to delay values as a bit-time percentile.

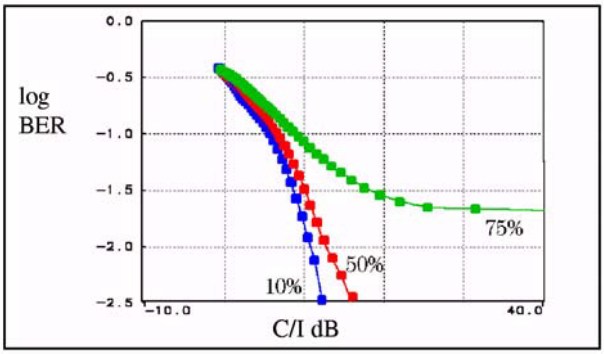

Figures 9d: BER vs. C/I for different 2nd ray delay values.

The second BER example simulates a GSM system including the OMSK modulator and a coherent GMSK demodulator. The GMSK modulator consists of a Gaussian filter, and an FM modulator with a sensitivity of 1/(4STIME) Hz/volt where STIME is the input data bit time. The input bits are first hard limited into an NRZ format. The 3-dB bandwidth of the Gaussian filter is set to 0.3/STIME (0.3 GMSK). The demodulator is a suboptimal coherent GMSK with built in carrier and clock recovery scheme. The propagation channel is one of the GSM options (rural area) with six taps and a delay profile with a maximum delay of 0.6 microseconds. This corresponds to about 16% of the

symbol duration (3.7 microseconds). Longer delay profiles (like hilly terrain in GSM) would require equalization. The propagation channel includes both flat and frequency-selective fadings.

Figure 10a shows the schematic representation of the design including fading radio channel with CCI channel as well as the desired signal. Figure 10b depicts the BER vs. C/I for three different mobile velocities (10, 25 and 50 km/hr) corresponding to Doppler frequencies 8.3, 20.8 and 41.7 Hz at 900 MHz. Finally, Figure 10c shows the BER results for different propagation environments as specified in GSM standards. This result shows that in the absence of equalization, poor BER results are obtained for urban and hilly terrain (where delays are much longer than bit duration).

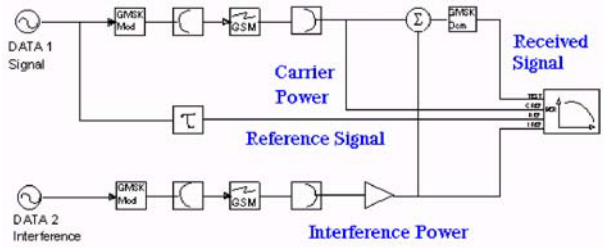

Figures 10a: GSM system including a fading radio channel with CCI.

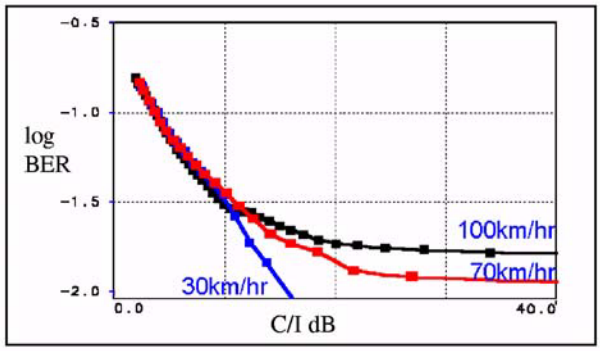

Figures 10b: BER vs. C/I in GSM propagation channel for different mobile speeds.

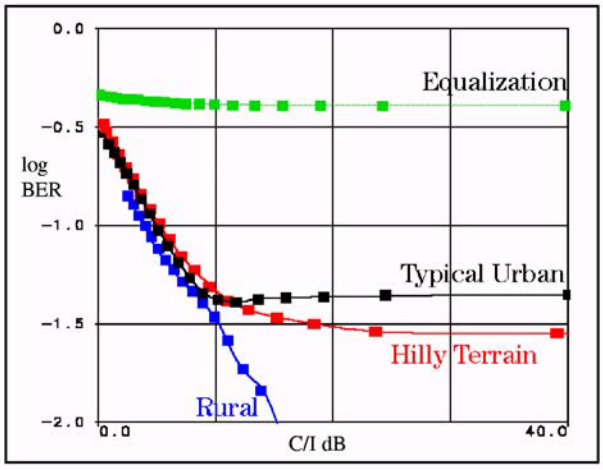

Figures 10c: BER in different environments.

Conclusion

System simulation is a powerful tool for the analysis and design of communication systems. The simulation of the radio channel is particularly worthwhile due to the otherwise extremely laborious and costly measurements. A simulation environment where the radio channel blocks are integrated with circuit, behavioral, and DSP models, allows the designer to study the interaction of radio, modulation, and digital channels simultaneously. Simulation of realistic mobile/portable scenarios where propagation takes place in uncoordinated, overlapping networks of interfering transmitters is clearly a desirable feature. Antenna and propagation modeling should be compatible with such realistic scenarios when due consideration is given to effects such as mobile travel and distance-dependent pathloss. Compatibility with industry standard such as GSM, allowance for fading, time and frequency spread and various faded signal distributions are also advantageous.

In this article, radio channel models consistent with above requirements were used, and a number of applications, including the impact of changing C/I on signal quality and the degradation of BER due to interference proximity were simulated. Also, using these radio channel models, a diversity combining scheme was shown to improve fading margins.

REFERENCES

Steele, Raymond, 1992.-"Mobile Radio Communications", Pentech Press,.

Hata, M., 1980. "Empirical Formula for Propagation Loss in Land Mobile Radio". IEEE Trans. VT-29, pp. 317-325.

Okumura, Y., 1968 "Field Strength and its Variability in VHP and UHF Land Mobile Service." Review of Electrical Communication Laboratory, Vol 16, pp. 825-873.

GSM 05.05 1974.Recommendation, Radio Transmission and Reception.

Jakes, W. C. (Editor),1974 Microwave Mobile Communications, John Wiley & Sons

YELENA CHAIKO was born in Riga, Latvia and she studied at Riga Technical University, Transport Communications and Information Systems professor group and obtained her degree in 2004. She works at Riga Technical University Her e-mail address is : krivcha@inbox.lv.